Different ways of reducing vibrations induced by cryogenic instruments

J.L. Lizon*[a], G. Jakob [a], B. de Marneffe[b], A. Preumont[b]
[a]European Southern Observatory, Karl-Schwarzschild-Strasse 2, 85748 Garching bei München, Germany;
[b]Université Libre de Brussels CP165/42, av. F.D. Roosevelt, 50
B-1050 Brussels, Belgium

ABSTRACT

The infrared instruments and most of the detectors have to be operated at cryogenics temperatures. Today, this is generally achieved using mechanical coolers. Compared to traditional nitrogen systems, these coolers, which large implementation started 15 years ago, have the advantage of reducing considerably the operation effort at the observatories. Depending of the technology, these coolers are all generating a level of vibration which in most of the cases is not compatible with the extremely high stability requirement of the large size telescope.

This paper described different ways which have been used at ESO to reduce the vibration caused by the large IR instruments. We show how we reached the goal to have the cryogenic instruments so quiet that they do not affect the operation of the interferometry mode of the VLT. The last section of the paper reports on a unique system based on a counter vibration principle.

Keywords: Vibrations, Cryo-cooler, Interferometry

1. INTRODUCTION

When the VLT and the VLT instrument program were launched it was known that vibration will be an issue. The VLT intreferometry program was already defined but its schedule was well behind the completion of the first instruments. If it was clear that vibration could disturb the operation of the VLT-I it was not easy to predict the exact impact. It was also not possible to define clear specifications on the acceptable level of vibration. The instrumentation teams took the necessary care to reduce as much as possible the vibration but without real guide lines. The real amplitude of the problem came out when the VLT-I started operation, then it was time to envisage some drastic corrective actions. This paper described some of them.

2. HISTORIC, BACKGROUND

The first mechanical cryo-cooler was introduced at ESO in 1990 to cool the detector of IRSPEC a near infrared spectrograph. This instrument, which was already in operation since 1983 on our 3.6 m telescope, was cooled with liquid nitrogen. In 1990 while transferring IRSPEC to the NTT we also upgrade its detector from a linear array to a first 32 x 32 pixel square array. It was also the occasion to upgrade the detector cooling from pumped liquid nitrogen to a Closed Cycle Cooler. The aim of this change was mainly to suppress the rather heavy operation that was the refilling of the detector cooling tank. Finally this turned out to be a very successful experience.

In a few years the philosophy to build cryogenic instrument changed completely and CCC were already adopted as the normal standard way to cool cryogenic instruments. In 1992, while starting the VLT program a survey were done in order to select "the" standard cryo-cooler for the range 65K/15K. The Leybold/Oerlikon machine was selected at this time for its simplicity and compactness. Thanks to its pneumatic drive (the displacer is free flying pressed driven by the helium) this cooler offer a cooling power 20% higher than a mechanically driven cooler. On this machine the maintenance which is extremely easy can even be done (with some cares) at cryogenic temperature. For all these attractive reasons, the RGD 5/100 cryo-cooler was selected to equip the VLT near infrared instrument.

*jlizon@eso.org; phone 0049 8932006780; fax 0049 8932006457; www.eso.org

In parallel an Anti-Vibration mount using bellows and counter spring was designed in order to reduce the impact of the Closed Cycle Cooler head on the instrument. ISAAC, the first VLT Infrared instrument was built under these conditions. Years of operation has shown that, even at the highest resolution mode, the performance of this instrument is never affected by the vibrations of its cryogenic system. The first warning came a few years later with the installation of CONICA. CONICA is a near Infrared imager spectrograph which is coupled to a large adaptive optic system (NAOS) to give a diffraction limited facility called NACO. Some extreme modes of this instrument combination are clearly affected by vibration transferred onto the AO components. The most important worry came when the VLT started to be operated as an interferometer. All these measures, which had allowed building instruments which are not suffering from their own vibrations, were clearly insufficient for the high demanding VLT-I mode of the VLT. In 1998 the vibration problem was so acute that a large anti-vibration plan was launched.

3. HAWK-I CASE

HAWK-I (High Accuracy Wide filed K Imager) is a near Infrared imager which is operated up to the K band. In the original version, two cold heads are used to keep the instrument at cryogenic operating temperature. The first stages of both heads are used to heat sink both the optical assembly and the radiation shield. The second stage of one head is used to cool the detector mosaic while the second one is connected to the sorption pump.

Due to the important impact of vibration, a special tool called Manhattan2 (MN2) has been deployed on the VLT. MN2 consists in a set of 8 accelerometers placed at strategic position on every UT. Four of those accelerometers are actually placed around the M1 at ~90°. One is placed on the top of spider interface to M2 unit. Two are placed on the interface plate of the M3 (interface to tower side). The last one is positioned on the arm of the M4 mirror. The vibration signals are then converted into optical path difference (OPD). The global OPD introduced in the light path is then compensated at the delay lines (DLs) level. The MN2 system can be used in standalone to determine the sources of vibrations and their level. The results presented in this chapter have been obtained on the telescope UT4 using MN2. The global piston on each mirror will be the metric used here to judge the levels of vibrations.

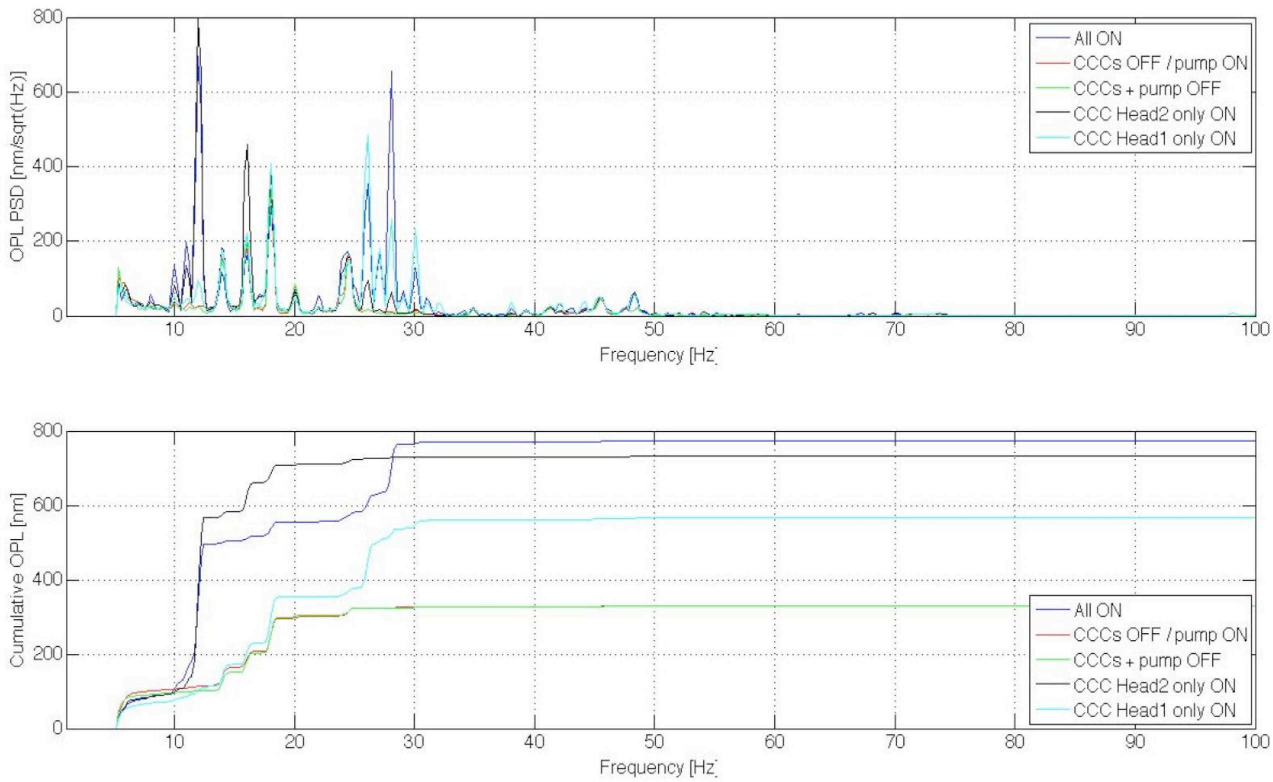

Figure 1: Vibration level of HAWK-I original configuration

Even if the general level of the UT vibration is already high, the contribution of HAWK-I is much higher than the maximum allowed for VLT-I operation. Two groups of frequencies are mainly generated by the CCCs: A strong peak at 12 Hz and another group of frequencies around 27 Hz.

If we consider that the vibrations contributions are uncorrelated between the different contributors, then we have:

$$\sigma^2_{Total} = \sigma^2_{HAWK\text{-}I} + \sigma^2_{Tel} \tag{1}$$

Where σ^2 are the OPD rms, and σ^2_{Tel} represents the contributions to the telescope of the other sources than HAWK-I, i.e. the level hen the HAWK-I CCCs and pump are off.

We have then $\sigma_{HAWK\text{-}I} = \mathrm{sqrt}(778^2 - 332^2) = 704$ nm

A detail analysis of the transmission of the vibration directly at the source is required. Figure 2 shows the AV mount used on HAWK-I. This is an upgraded version of the original design where the counter springs have been replaced by four evacuated bellows. This allows a significant reduction of the rigidity of the AV mount and in consequence a reduction of its Eigen frequency.

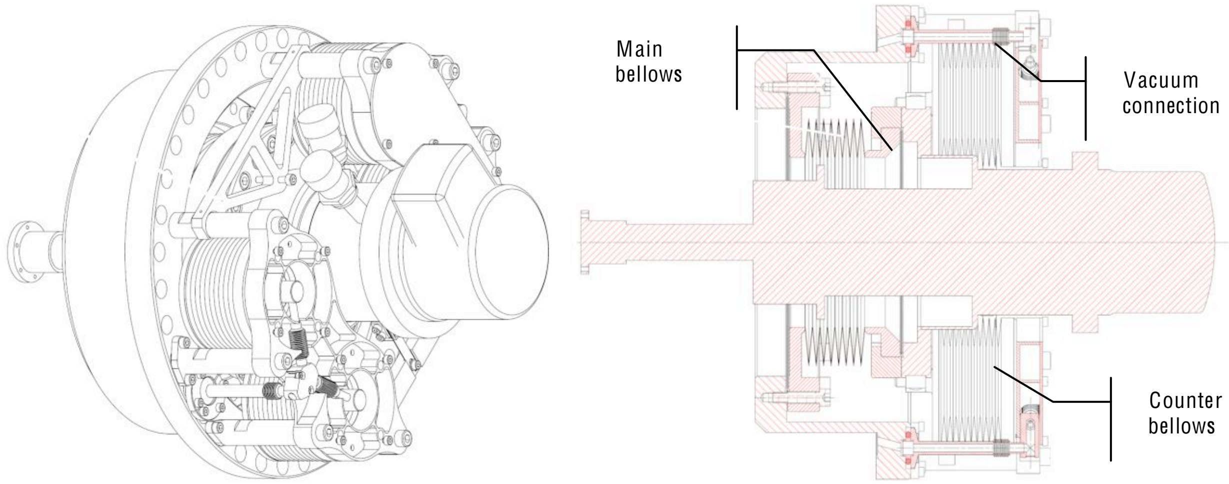

Figure 2: CCC anti-vibration mount

The CCC cold head is mounted on a membrane bellows in order to be cinematically decoupled from the vessel. Four counter bellows are used to compensate the differential pressure and then avoiding the collapse of the main bellows. Two small tubes systems are used to link the counter bellows to the main vacuum. This allows the cold head to be freely suspended on an elastic system having a resonance frequency of a few Hz.

Table 1 shows the results of a series of measurements carried out in various configurations to try to identify more precisely the origin of the problem.

Measurements	Configurations	OPD (nm rms)			
		M1	M2	M3	Tel. Tot
1	Air (thermal links out)	169	124	271	297
2	Vacuum (thermal links out)	205	169	221	400
3	Vacuum (thermal links connected)	480	350	550	630

Table 1: Vibration transfer analysis

Measurement 1 has been taken with the instrument open and the cold head suspended on the AV system. This demonstrates clearly the efficiency of the dumping system.

Measurement 2 shows a clear degradation while the system is used under vacuum. This is mainly due to the large difference between forces acting on each side of the bellows.

Measurement 3 shows a further degradation after the connection of the thermal links. In this type of system the thermal wicks have to be sized in order to transfer some 100 Watts. An effective thermal conductance results of delicate optimization of the length and cross section which is not favorable to a high flexibility. The high flexibility of the AV mount also causes larger motion of the head. For a given spring constant the thermal link induced larger forces on the instrument.

Thanks to its domain of operation and to its design, a way to improve this instrument was rather easy to find. With a wavelength coverage up to the K band, HAWK-I does not need to be operated at extreme cryogenic temperature. An optical system at 140 K would already ensure the optimal performance and a sufficiently low dark current.

HAWK-I is also fitted with a standard ESO LN2 continuous flow system for the pre-cooling. Figure 3 shows the circuitry of the liquid nitrogen pre-cooling system. The instrument is cooled by 5 sub-circuits supplying the various heat-exchangers distributed all over the complete optical assembly. Two additional heat exchangers (marked in red in the right view) were added to cool the radiation shield which, in the original version, was only cooled by the CCCs. These two additional heat exchangers have been introduced in series in the entrance of the two cold structure sub-circuits. A rotating feed-through developed for a previous application allowed supplying the instrument in LN2 even during operation. This was enough to convert like this the pre-cooling system in the operational cooling system. Only one CCC head has been kept to cool the detector mosaic to its optimal operation temperature of 65 K.

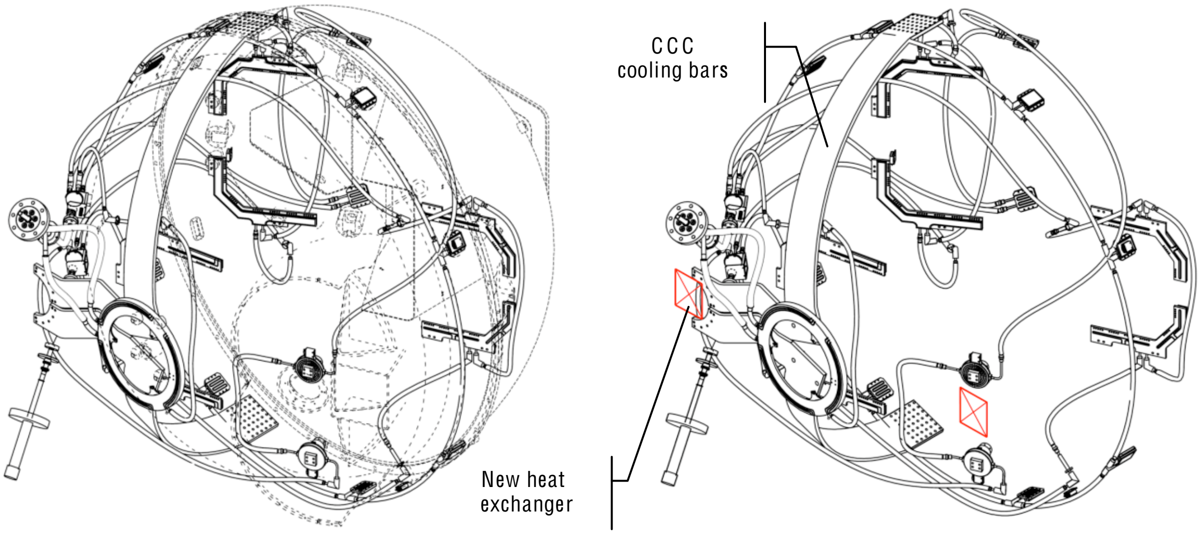

Figure 3: 3D view of the HAWK-I pre-cooling system

Figure 4 shows a vibration measurement recorded right after the modification. The result is excellent and the HAWK-I vibration contribution computed using the equation (1) has been reduced to some: $\sigma_{HAWK\text{-}I}$ = 230 nm

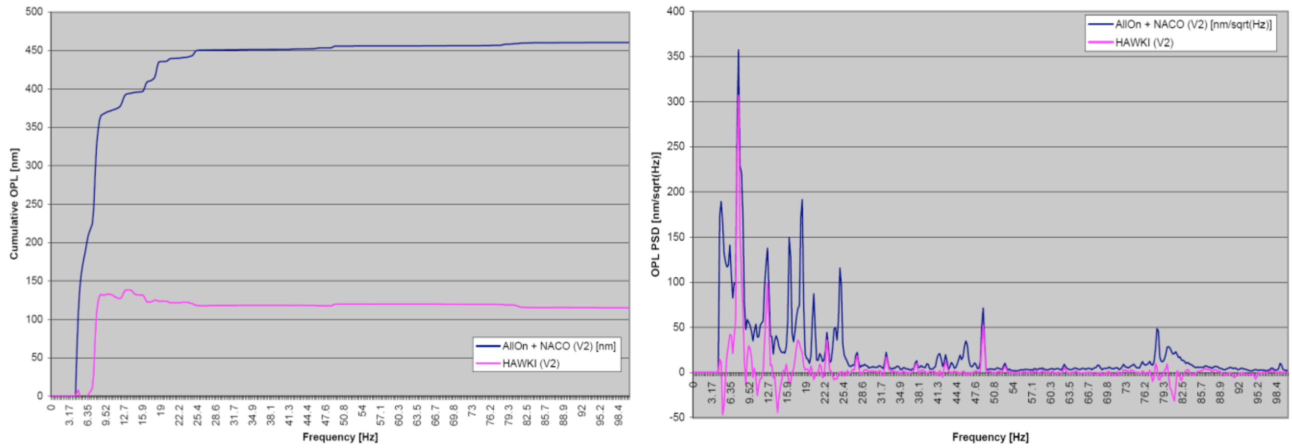

Figure 4: Vibrations introduced by HAWK-I after the modification

4. CRIRES CASE

CRIRES (CRyogenic InfraRed Echelle Spectrograph) is a high resolution infrared spectrograph operating in the 1 to 5 micron wavelength range which is fed through an AO module. Figure 5 shows a view of the arrangement on the Nasmyth platform. The spectrograph (~570 Kg cold mass) is packed in a 2.5m diameter vacuum vessel which is supported and aligned behind the AO module. This extremely massive system (total of 4500 Kg) is directly bolted onto the Nasmyth platform.

A negligible background emission can only be obtained when the optic assembly is operated around 70K or below, a temperature which cannot be reached in a standard way with liquid nitrogen. The original designed used 3 of the pneumatically driven CCC heads. Two of them are installed with main axis horizontal axis around the upper cylinder of the vacuum vessel. A third one, installed with vertical axis on the bottom of the vessel, is accessible through the large opening of the supporting structure.

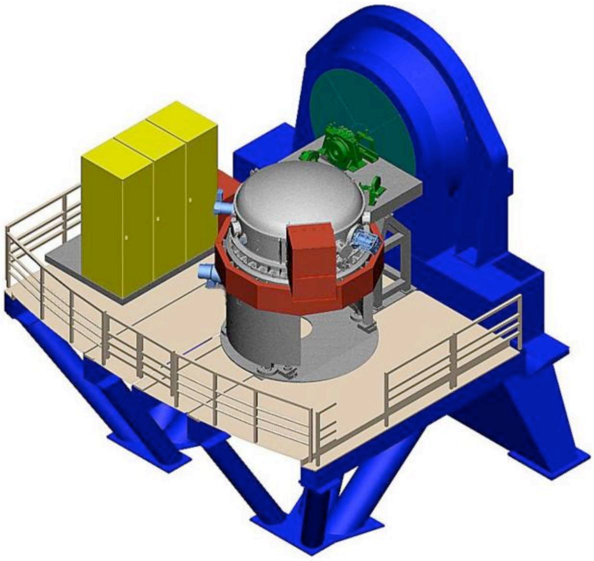

Figure 5: CRIRES arrangement on the Nasmyth platform of VLT UT1

For this specific application and the temperature range required, there was no way to avoid cryo-cooler. Fortunately the large survey and test campaign launched (in the frame of the anti-vibration plan) to select a "low vibration" high power machine pointed out the Cooler 10 MD from Leybold Oerlikon as having a significantly lower level of vibration. High priority was given to the preparation of an up-grade of the instrument with this machine. A new adaptation of the AV mount (shown in figure 6) was necessary to accommodate this much larger cold head. A thin steel cable (not shown on the figure) is used to support vertically the 22kg heavy new head.

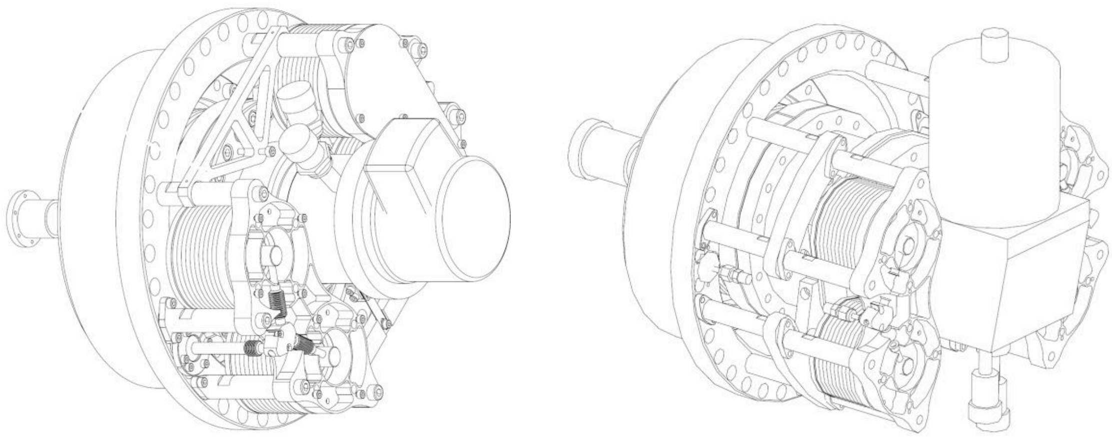

Figure 6: AV mounts comparison

MN2 has been used to evaluate the gain obtained after the modification in January 2009. Figure 7 shows the vibration tracking sheet from Paranal. These changes brought CRIRES at very low level of contribution: $\sigma_{CRIRES} < 100$ nm

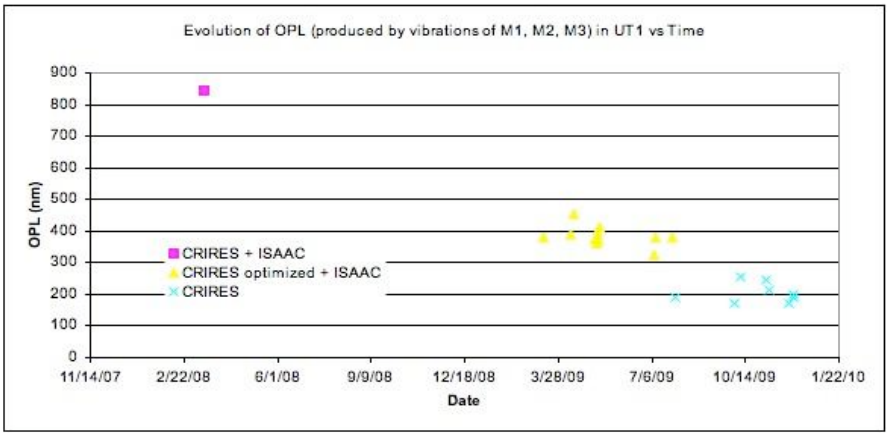

Figure 7: Vibration tracking data sheet (courtesy from P Hagenhauer)

5. COUNTER VIBRATION SYSTEM

In the emergency it was decided to attack the vibration from all possible sides. We have already described the remedy to the problem applied to two specific cases. In parallel to these specific improvements the anti-vibration plan foresees also the development of a counter vibration system which can canceled the vibration induced by the CCC head.

The aim of this was to try to develop an active vibration cancellation system that reduces the impacts of the cooler's vibrations. The cancellation system is based on a proof-mass (inertial) actuator equipped with a voice coil transducer and an acceleration sensor. In our case, the displacer is pneumatically actuated, which makes the situation even worse as the vibrations are no longer harmonic but instead caused by impact shocks. The shocks occur when the displacer hits the limits of the cold head's inner space. It is explained below that the classical feedback controllers have very limited effects in our case, which is why we use specific controllers based on the repetitiveness of the disturbance. Many of such controllers exist in the literature, but not all of them can handle the many harmonics that result from the repetitive impacts. In this work we have been comparing three controllers that seem to meet our requirements, namely the filtered-x LMS, the harmonic control and the Repetitive Control based on the Internal Model Principle.

The cryo-cooler is schematized in Figure 8 (left), with its displacer that moves back and forth with a period time of 1s. The cooler is placed on a soft suspension, the AV mount. If the cooler is considered to be rigid, it can be reduced to the single system shown in Figure 8 (middle), where M = 12.5 kg is the mass of the cooler, k ~ 27.5 kN/m is the stiffness of the suspension, and the disturbance $d(t)$ represents the reaction forces exerted on the cooler by the displacer during each impact. The corner frequency of the suspension was measured to be about 7.5 Hz. No damper is actually introduced in it, so that it is very lightly damped (ζ ~ 0.2%).

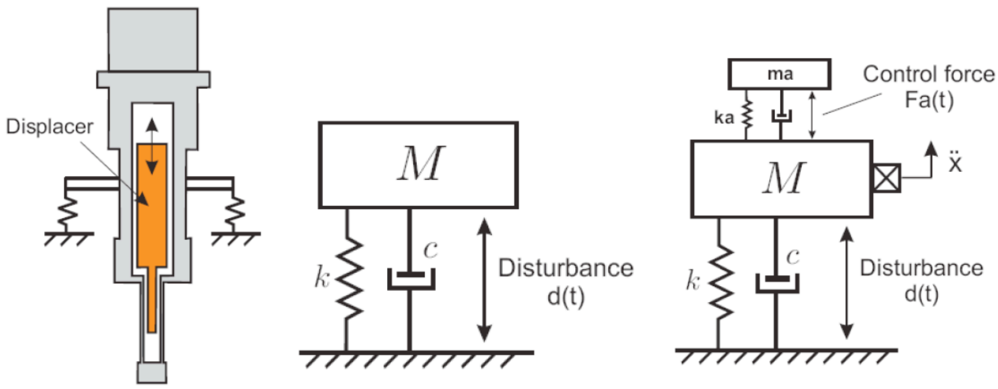

Figure 8: CCC model (left: cooler with displacer, middle: cooler model, right: control system)

In order to design the control system we have to find a signal $d(t)$ which is sufficiently representative (in terms of frequency decomposition, peak amplitude, and repetitiveness) of the "real" force exerted by the displacer. Because we do not have access to the inside of the cooler we are obliged to guess what is happening in it. The simple approach taken here is based on the observation that the acceleration signal (see figure 9) is made of 3 sharp peaks followed by free oscillations of the spring-mass system,

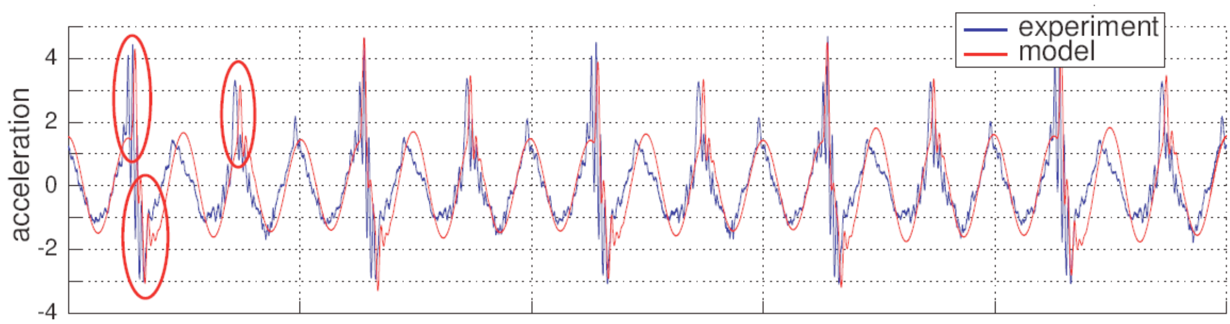

Figure 9: Experimental and numeric acceleration of the cryo-cooler filtered at 100Hz

Accordingly, we tried to model d(t) as a series of periodic pulses, with each pulse placed at the position of one peak. Physically, the pulses correspond to the impacts of the displacer against the cold head. The position, amplitude and duration of each pulse were chosen in such a way that the resulting vibration of the cold head is as close as possible to that observed experimentally, both in the time domain and in the frequency domain. The results in time domain are shown in figure 9 (red curve) the correlation with the experiments is very good. The results are somewhat less good in the frequency domain, as shown in figure 10, which plots the experimental and numerical cumulative Mean-Square acceleration.

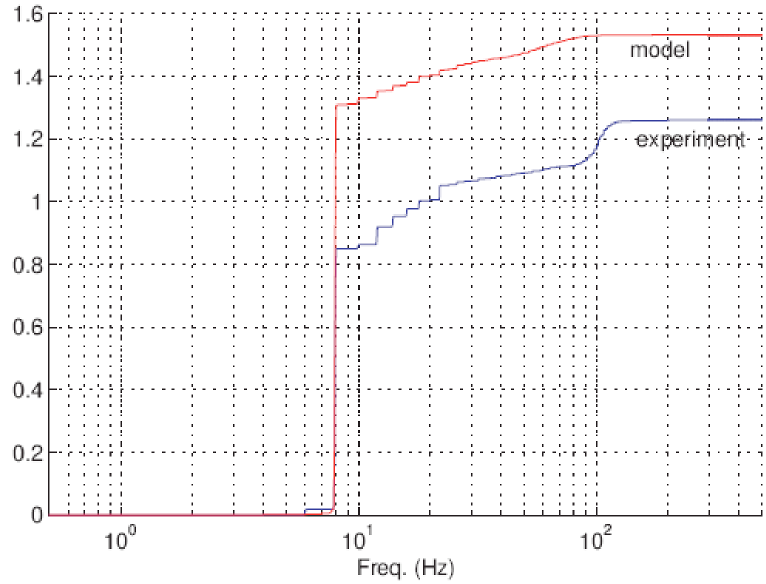

Figure 10: Experimental and numerical cumulative Mean-Square acceleration of the cryo-cooler (in $(m=s/2)^2$).

The model overestimates the amplitude of the harmonic at 8 Hz and underestimates the amplitude of those at other frequencies; this conflict is due to the simplicity of the model, which has too few parameters to allow us to fix the amplitude of each harmonic independently. In spite of this, the model correctly predicts the order of magnitude of each harmonics as well as the frequency region where the disturbance is present, which is what we are really looking for the design of the control system (in terms of bandwidth, power, stroke, etc.). Moreover, it was observed that the frequency behavior of the cooler can change from one day to the other, so there is no point in trying to model it very precisely.

The control system is schematized in Figure 8 (right): a reaction mass ma (~ 2 kg) is placed, through a soft suspension (k_a,c_a) on top of the cooler, and a pair of opposite forces $F_a(t)$ is exerted on M and on ma by means of an electromagnetic transducer. The absolute acceleration x(t) of the cooler is measured with a piezoelectric accelerometer. The resonance frequency ω_a = of the inertial actuator should be lower than 1 Hz (the frequency of the disturbance) so that it behaves as an ideal point force transducer at all the frequencies that we wish to control. Such a low frequency is however very difficult to achieve, if only because a very soft stiffness ka leads to a very large static deflection of the transducer, so we were forced to take it ten times higher (i.e. approximately equal to the suspension frequency of the cryo-cooler). This brings acceptable values of the static deflection, but the price to pay is a larger control effort $F_a(t)$ and a larger deflection at all frequencies below ω_a, and more difficulties when designing the feedback controller. Note, on the other hand, that as the frequencies of the actuator and that of the structure are similar, the actuator behaves like a Mass Damper and introduces some passive damping in the structure, which is favorable.

The easiest way to control the vibrations of the cold head consists in implementing a classical feedback controller H(s) linking the measured acceleration x(t) to the force input $F_a(t)$. After some trial and errors a suitable controller was found. Although the classical feedback controller somewhat improves the situation, it is clearly not enough, which is why we decided to add a second control layer, using this time algorithms specifically developed for periodic disturbances. Three different types of algorithm have been tested as second control level.

The so-called Filtered-x LMS (Least Mean Squared) algorithm is widely known, and its adaptation for the case of periodic disturbances is rather common. The principles of the Fx-LMS are shown in figure 11. A reference signal x is sent to a FIR filter F whose output is the command signal u of the actuator. F is adapted at each time step until the measured error e reaches a minimum.

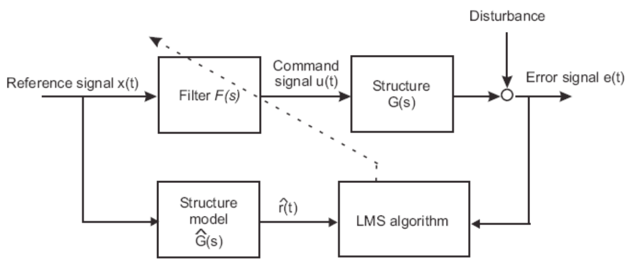

Figure 11: Principle of the Filtered-x LMS

The classical Fx-LMS described previously is effective, but it lacks any frequency selectivity because it has only two tuning parameters (a and b). Instead we would like to have a frequency-tunable convergence rate, increasing it in some important frequency regions (or where the system is well-known and the stability is not an issue) and decreasing it or even suppressing it in other regions. If the disturbance is periodic this can be done with the so-called harmonic control (HC) shown in figure 12 (left). A signal generator sends a sum of sine signals to the control input of the cryo-cooler $F_a(t)$; the amplitude and phase of each sine is progressively adapted, based on the measured error e(t) = x(t), until e(t) has no component at the selected frequencies.

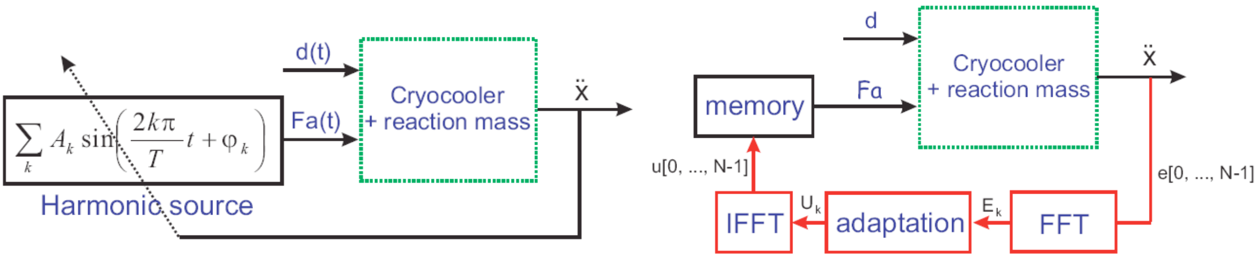

Figure 12: Principle of the Harmonic Control and HC for multi-frequency disturbances

If the system is linear the harmonics do not interact and the controller can be decomposed into a set of independent control loops. The technique is illustrated in figure 12 (right). The (discrete-time) error signal is recorded during one cycle: $e[0; \ldots; N-1]$. An FFT is executed on $e[0; \ldots; N-1]$, decomposing it into its complex harmonic E_k ($k = 0; \ldots; N-1$). The adaptation law is executed (once per harmonic), producing the complex amplitudes of the control force U_k. An inverse FFT is then performed on the U_k, so as to transform them into a time sequence u[0; ::: ;N ¡1] which is recorded in memory and executed during the next cycle.

The Repetitive Control (RC) is a feedback technique based on the Internal Model Principle, which states (loosely speaking) that any stable feedback system will ultimately suppress any disturbance on condition that a “model” of that disturbance is included in the feedback path. In our case the “model” of the disturbance consists of a periodic signal generator obtained by inserting a time delay z^{-N} inside a positive feedback loop, as shown in figure 13. According to that figure, the error signal is first filtered through $L(z)$, next delayed by $N = T{=}Ts$ sample times, and finally sent to the periodic signal generator.

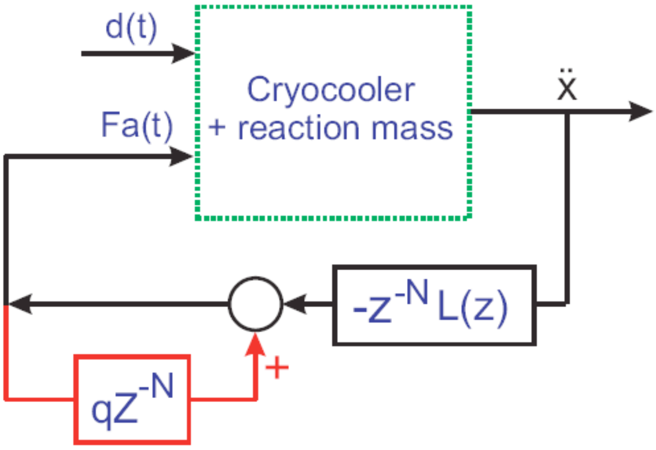

Figure 13: Principle of the Repetitive Control

The concept has been experimentally verified first on the small-scale laboratory demonstrator shown in figure 14. It is build according to the model of Figure 8 (right), that is, a small reaction mass m_a is connected, through a soft suspension, to a larger mass M representing the cooler. The suspension connecting the cooler to the ground is introduced by means of two flexible bearings, which are also used to guide M and ensure an axial movement. An electromagnetic actuator (“magnet 1” and “coil 1”) is used to introduce the disturbance $d(t)$. A soft spring connects m_a and M, and coaxial displacement is ensured by the use of a ball bearing: the option “spring and ball bearing” was preferred to the use of flexible bearings because the relative displacement between the two masses might be quite large (±6mm). A second moving coil transducer is used to introduce the control force $F_a(t)$, and an accelerometer measures the movements of M. The reaction mass m_a is well damped thanks to the eddy currents that appear in the metallic support of coil 2.

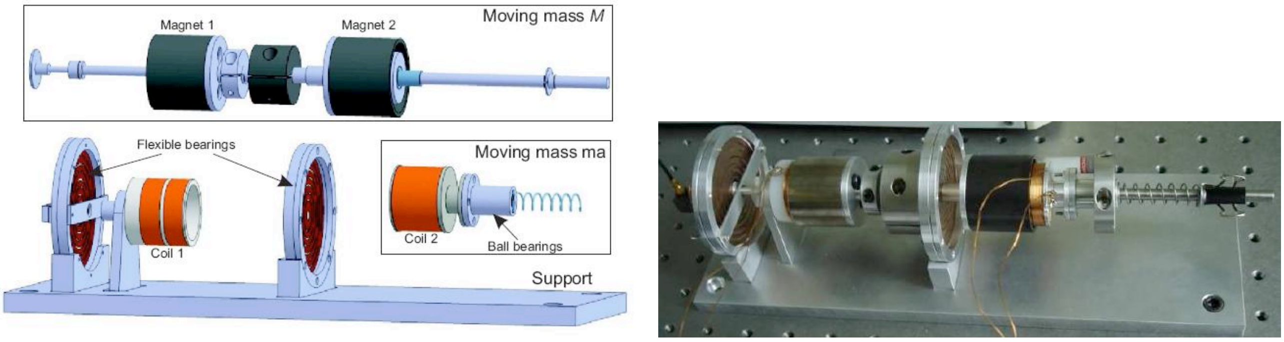

Figure 14: Small scale laboratory demonstrator

Experimental displacement signals are shown in figure 14 (left), and figure 14 (right) plots the cumulative Mean-Square displacement. It is found that the three “periodic” algorithms have the same performances and very efficiently attenuate the repetitive disturbance: for each controller the displacement signal after convergence is mainly composed of the harmonic at 1 Hz, which we do not want to control because it requires unacceptably large control input. In particular, the Mean-Square displacement is divided by 30 with respect to the case “classical feedback only” and by 90 with respect to the case “control off”. (Note that, because the actuator introduces some damping, the response without control is itself lower than that without actuator). The fact that the three controllers have the same performances is easily explained by the observation that the main contribution to the cooler’s displacement is in the range [6- 18] Hz, and then well within the bandwidth of each controller.

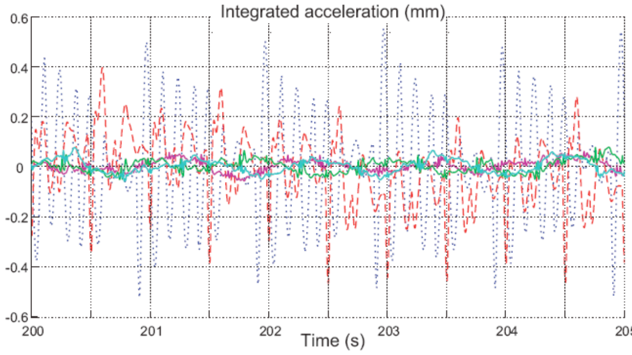

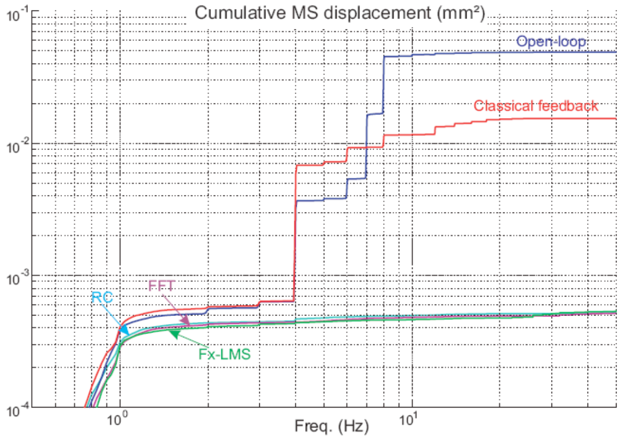

Figure 15: Experimental displacement of M and experimental cumulative Mean-Square displacement for various controllers
Dotted: control OFF; dashed: classical feedback only; plain: classical feedback + specific controller (Fx-LMS, RC, harmonic control).

Figure 16 shows the first inertial actuator prototype which has been build in order to test the principle on a real CCC head. This arrangement has been chosen in order to reduce the length to a minimum, using available parts out of high density tungsten.

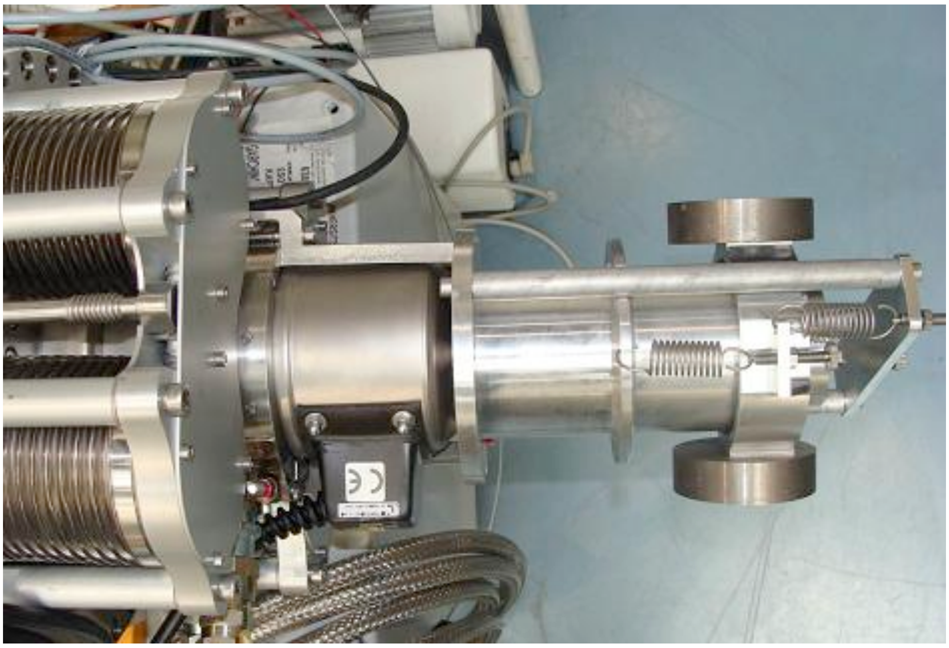

Figure 16: CCC cold head actuator

The determination of the frequency response of the system required a number of averages and shows a very low value of coherence function, particularly in the 10-20 Hz range. This indicates a lot of non linearity. An anti-resonance was also detected (at 8 Hz): that frequency will be difficult to control, because the control system has very limited effect at such frequencies. The appearance of anti-resonance is due to the fact that the system is not uni-axial. Because of the anti-resonance and of the light damping of the system, the phase changes abruptly at 8 Hz: imagine that the position of the anti-resonance slightly change with time, and the change in phase might exceed 90° which would make the system unstable. Because of this it was decided to decrease the value of α corresponding to 8 Hz by a factor 10, and so did we for the frequencies 11 to 16 Hz. The testing was done under these conditions.

The resulting acceleration signal x_f is shown in figure 17 (the time and in the frequency domain), and the control signal V_a is shown in figure18. Most of the harmonics until 50 Hz are effectively suppressed, except for the 8 Hz harmonic. It is also seen in figure 17 that the time signal (right column) does not change much: this happens because the acceleration $x_f(t)$ has a very large frequency spectrum, and we control only the first 50 harmonics of it. By contrast, the displacement of the cold head has a much more limited frequency spectrum, and simply by looking at the cooler it could be verified that the displacement of the cold head was effectively attenuated.

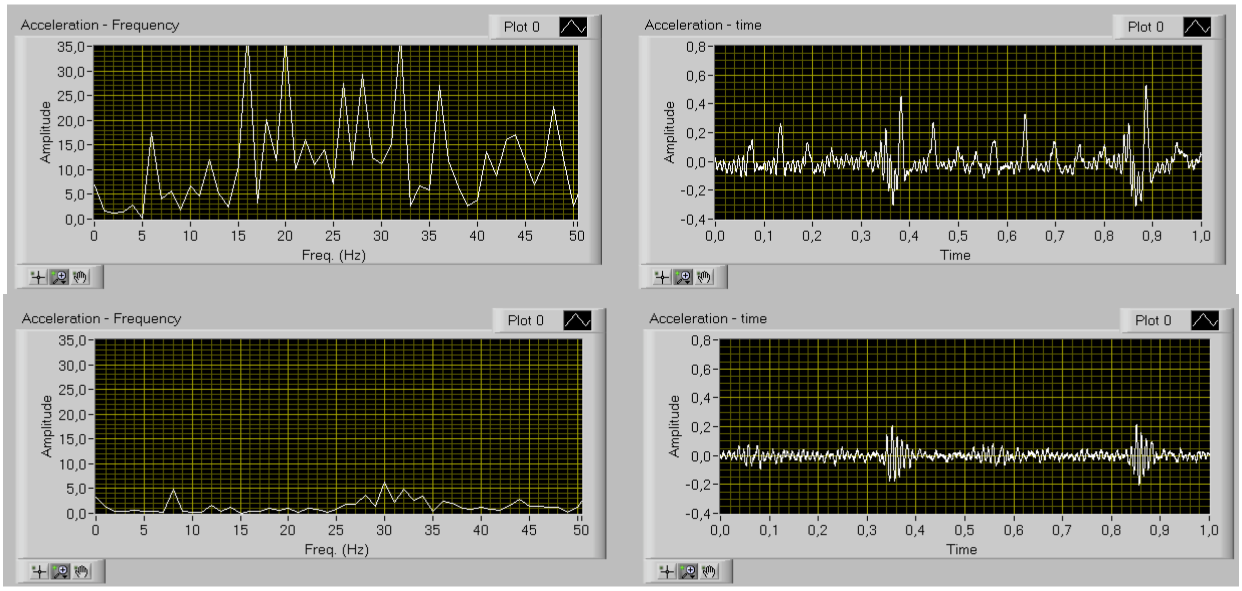

Figure 17: Uncontrolled (top) and controlled (bottom) acceleration of the cold head.

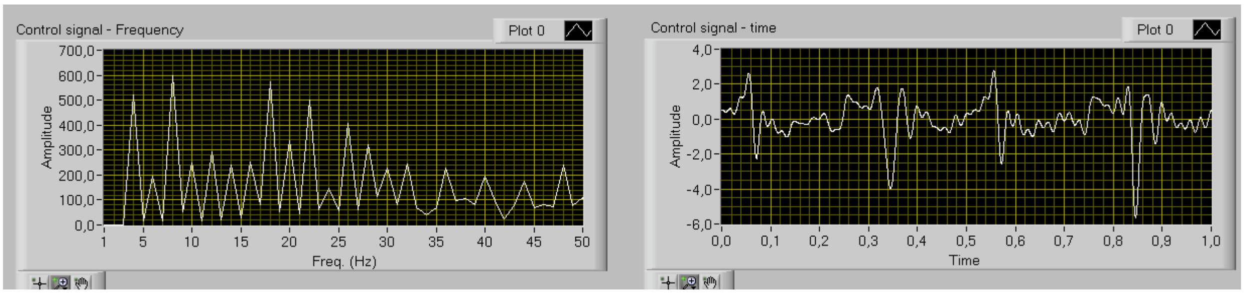

Figure 18: Typical control signal $V_a(t)$

The promising results recorded in the laboratory have still to be confirmed on the VLT. A test campaign is already scheduled for late 2010. Unfortunately the range of application of this system will still be very limited. Only CCC used with the main axis remaining horizontal can benefit from this device. It will never support a design with an axis rotating relative to the gravity.

6. CONCLUSION

The main conclusion from all this work and other additional work around the reduction of the vibration is: The best is not to produce any vibration in a telescope environment. Cooling system for instrument to be used on telescope operating in interferometric mode should be chosen such that they produced the minimum of vibration. Depending of the nature and design characteristic of every project, the fastest up-grade solution has been chosen. Despite the good results recorded with CRIRES and HAWK-I we should not forget that this is still relative. These two instruments are now just back inside the general vibration noise of the VLT which is rather high. Any further improvement of the telescope infrastructure would make them pointing as potential problem.

AKNOLEDGEMENTS

The authors would like to thanks the VLT-I colleagues from Paranal for their patience in waiting for viable solutions. Among of them we would like to thanks more specially P.Hagenauer, S Poupar and P Gitton for their permanent availability for measuring and analyzing any new ideas. The authors warmly thank G. Pinte from the Flanders' Mechatronics Technology Centre (FMTC) for his time and useful explanations when developing the Repetitive Control system.

REFERENCES

1. http://www.eso.org/sci/facilities/develop/integration/
2. Kaeufle, H., Ballester, P., "CRIRES: a high-resolution infrared spectrograph for ESO's VLT" Proceedings of SPIE Vol.5492, pp 1218-1227 (2004).
3. Casali, M., Pirard, J., "HAWK-I: the new wide-field IR imager for the VLT" Proceedings of SPIEVol.6269, 62690W (2006).
4. C. Kempf, W. Messner, M. Tomizuka, and R. Horowitz Comparison of Four Discrete-Time Repetitive Control Algorithms, IEEE, Control Systems Magazine, Dec. 1993, pp.48-54.
5. C.R. Fuller, S.J. Elliott, P.A. Nelson Active Control of Vibration, Academic Press, 1996.
6. S. Elliott, Signal Processing for Active Control, Academic Press, 2001.
7. G. Pinte, Active Control of Repetitive Impact Noise, PhD Thesis, KULeuven, 2007.
8. A. Preumont. Vibration Control of Active Structures: and Introduction. Kluwer, 2002. 2nd edition.
9. B. Stallaert, G. Pinte, S. Devos, W. Symens, J. Swevers, P. Sas; Filtered-X LMS vs repetitive control for active structural acoustic control of periodic disturbances. Proc. ISMA 2009, Leuven.